Investigation of Sequence Isomer Effects in AB-Polybenzimidazole Polymers

Alexander L. Gulledge,[1] Xiaoming Chen,[2] Brian C. Benicewicz[1]

[1]Department of Chemistry and Biochemistry and USC NanoCenter, University of South Carolina, Columbia, South Carolina
[2]Department of Chemical Engineering, University of South Carolina, Columbia, South Carolina
Correspondence to: B. C. Benicewicz (E-mail: benice@sc.edu)

Received 1 October 2013; accepted 18 November 2013; published online 30 November 2013
DOI: 10.1002/pola.27037

ABSTRACT: In the present work, a unique series of random polybenzimidazole (PBI) copolymers consisting of the recently reported novel isomeric AB-PBI (*i*-AB-PBI) and the well known AB-PBI were synthesized. The *i*-AB-PBI incorporates additional linkages (2,2 and 5,5) in the benzimidazole sequence when compared with AB-PBI. Random copolymers, varying in composition at 10 mol % increments, were synthesized to evaluate the effects of sequence isomerism in the polymer main chain without altering the fundamental chemical composition or functionality of a polymer chain consisting of 2,5-benzimidazole units. Polymer solutions were prepared in polyphosphoric acid (PPA) and cast into membranes using the sol–gel PPA process. The resulting polymers were found to have high inherent viscosities (>2.0 dL/g) and showed elevated membrane proton conductivities (~0.2 S/cm) under anhydrous conditions at 180 °C. Fuel cell performance evaluations were conducted, and an average output voltage ranging from 0.5 to 0.60 V at 0.2 A/cm^2 was observed for hydrogen/air at an operational temperature of 180 °C without applied backpressure or humidification. Herein, we report for the first time glass transition (T_g) temperatures for AB-PBI, *i*-AB-PBI, and an anomalous T_g effect for the series of randomized PBIs. © 2013 Wiley Periodicals, Inc. J. Polym. Sci., Part A: Polym. Chem. **2014**, *52*, 619–628

KEYWORDS: AB-PBI; *i*-AB-PBI; fuel cell; gels; glass transition; high temperature materials; membranes; poly(2,5-benzimidazole); polybenzimidazole; PPA process; step growth polycondensation; structure-property relations

INTRODUCTION Polymer electrolyte membrane (PEM) fuel cells are clean energy conversion devices that have received much attention as a promising alternative to combustion-based energy generating devices.[1] However, one of the limitations associated with PEM fuel cells includes the availability and development of appropriate materials that would allow the cost of manufacturing these devices to compete with existing technologies.[2] One approach to overcome that limitation is developing more efficient PEM fuel cells. Fuel cell efficiency can be increased significantly by operating at elevated temperatures (>100 °C).[3] Higher operational temperatures have been shown to provide advantages such as faster electrode kinetics, increased resistance to fuel impurities[4] and simplified water and thermal management.[5] Moreover, to redeem the advantages of higher operational temperatures (>100 °C) in PEM-based fuel cells, a dopant other than water is required. Much research has gone into the development of alternative dopants for high-temperature PEM fuel cells, such as phosphoric acid (PA), and has been recently reviewed.[6]

Polybenzimidazoles (PBIs) are a class of aromatic heterocyclic polymers that are well known for their chemical and thermal stabilities under high temperature fuel cell operation conditions.[7,8] PBI is a basic polymer ($pK_a \sim 5.25$)[9] and possesses both proton donor and proton acceptor sites. These H^+ acceptor/donor sites of PBI allow for specific interactions with polar solvents such as PA.[10–12] These interactions have also been observed with other polymers as well, which gave rise to blending of PBI.[13–16] PBI polymers doped with PA are readily achievable and have been noted as a promising material for use as a polymer electrolyte in high temperature proton exchange membrane fuel cells.[17] PBI polymer membranes doped with PA used in PEM fuel cells are capable of operating at temperatures up to 200 °C because they do not rely on water for proton conduction.[18] Moreover, PBI membranes doped with PA have also been reported as promising candidates for low-cost and high-performance fuel cell materials.[17,20]

To date, a large variety of PBI polymers have been synthesized and studied in the literature,[6,21–25] however, PBI chemistry still remains an important area of interest in the high-temperature PEM fuel cell community. Many PBI variants containing a range of structural and functional moieties have been examined to further explore the effects of polymer

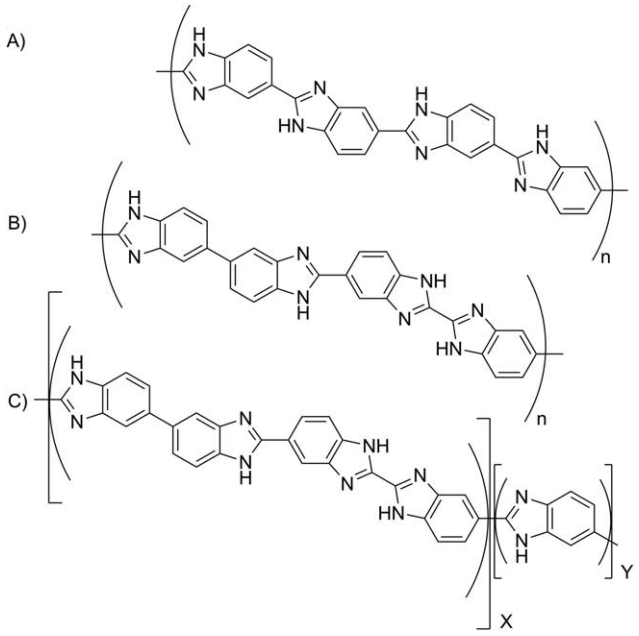

FIGURE 1 (a) Poly(2,5-benzimidazole) AB-PBI, (b) isomeric AB-PBI (*i*-AB-PBI), (c) random AB-PBI (r-AB-PBI).

structure on membrane properties.[13–29] Among these, several copolymer systems have been evaluated to extensively investigate how their properties change with respect to composition.[30–33] In this work, sequence isomerism in a unique copolymer system is evaluated.

We recently reported the synthesis of a novel isomeric AB-PBI, termed *i*-AB-PBI that was shown to have significantly improved properties resulting from a change in the benzimidazole sequence of the polymer, when compared with AB-PBI.[34] Herein we report the evaluation of random copolymers of various compositions between AB-PBI and *i*-AB-PBI. Isomerization of benzimidazole orientation in the *i*-AB-PBI allowed for direct comparison with AB-PBI and provided insights into the structure–property relationships of PBIs. Variation of composition in the random copolymers allowed for the direct study of how incorporation of various amounts of 2,2 and 5,5 linkages affected the properties of these materials by changing the main chain benzimidazole sequence. Figure 1 shows the structural repeat units incorporated in the AB-PBI, *i*-AB-PBI, and random AB-PBI. Membranes were prepared from the random copolymers using the PPA process[35] and were investigated to evaluate their proton conductivity and fuel cell performance properties. Thermal gravimetric analysis (TGA) and differential scanning calorimetry (DSC) were conducted to evaluate the thermal properties of these materials. Glass transition (T_g) temperatures were measured via dynamic mechanical analysis (DMA), and an anomalous T_g effect resulting from sequence isomerism was observed. The properties of the random AB-PBI membranes were compared to both AB-PBI and *i*-AB-PBI.

EXPERIMENTAL

Materials

Methyl-2,2,2-trichloroacetimidate (98%) was purchased from Acros Organics and used as-received. 2,2′-Bisbenzimidazole-5,5′-dicarboxylic acid (BBDCA) was synthesized and purified as previously reported.[34] TAB monomer, 3,3′,4,4′-tetraaminobiphenyl (polymer grade, ~97.5%) was donated by Celanese Ventures, GmbH (now, BASF Fuel Cell) and used as-received. PPA (116% concentration) was purchased from ThermPhos and used as-received. PA (85%) and common solvents (e.g., DMSO, MeOH, EtOH, etc.) were purchased and used as-received from Fisher Scientific. Purification of 3,4-diaminobenzoic acid (10 g, Acros, 97%) was conducted via recrystallization from water/methanol (480/160 mL) using activated carbon yielding pink/tan crystals after vacuum drying, 75%, m.p. 216.8 °C (Literature,[36] 210–211 °C).

Polymerization of Random AB-PBI Copolymers

In a typical polymerization procedure, 2,2′-bisbenzimidazole-5,5′-dicarboxylic acid, 3,3′,4,4′-tetraaminobiphenyl, 3,4-diaminobenzoic acid, and PPA were reacted on a 15 mM scale with various ratios dependent upon the targeted composition. Monomer concentrations in PPA were adjusted to reflect the homopolymer closest in composition to the targeted ratio. Monomers were then added to a 100 mL reactor. The reactor was then equipped with a three neck reactor head, a stir rod attached to an overhead stirrer and a nitrogen inlet/outlet. A slow nitrogen flow was established and monitored through an oil filled bubbler. The reactor was placed into an oil bath that was regulated using a temperature controller with ramp and soak features. The polymerization utilized the ramp/soak profile as follows:

An initial temperature of 60 °C was used, and the temperature was raised to 140 °C over a period of 1 h. The temperature remained at 140 °C for 2 h and was then increased to 180 °C over a period of 30 min. The temperature remained at 180 °C for 10 h, and was then increased to 220 °C in a period of 30 min. The reaction remained at 220 °C for the duration of the polymerization; 24–36 h was the typical duration of polymerization for the random copolymers. At the end of polymerization, PA (~15 mL) was back-added to the extremely viscous solutions to adjust the viscosity for subsequent membrane casting. Analysis: ^{1}H-NMR (400 MHz, DMSO-d6) δ 7.2–8.2 (broad multiplet, aromatics, 3H), 8.4 (singlet, 1H), 8.5 (multiplet, 2H).

PEM Preparation

After adjusting the viscosity with PA, the polymer solution was directly cast at 220 °C on to heated (120 °C) glass plates for membrane preparation. A heated metal casting blade (120 °C) with a casting thickness of 20 mil (508 μm) was used. After casting, the glass plates were separated and samples were placed into a humidification chamber maintained at a relative humidity of 55% at 25 °C. The polymer solutions were allowed to hydrolyze overnight. Hydrolysis of the PPA to PA induced a sol-to-gel transition that resulted in a Flory type 3 gel membrane.[37] The samples were then

sealed in 3 mil (76.2 μm) thick polyethylene bags until testing or membrane electrode assembly (MEA) fabrication.

Characterization Techniques

FT-IR spectra were recorded on a Perkin Elmer Spectrum 100 using an attenuated total reflection diamond cell attachment. ^{1}H-NMR were recorded using a Varian Mercury 300 spectrometer. TGA of dried polymer samples was conducted using a TA Instruments Q5000 with nitrogen or air flow rates of 25 mL/min and a heating rate of 10 °C/min. TGA was performed from room temperature to 750 °C. Mechanical properties were measured in tension using an Instron 5543A with an extension rate of 5.0 mm/min and were preloaded to 0.1 N at 3.0 mm/min using a 250 N load cell.

Inherent viscosity (IV) measurements were conducted using a Cannon Ubbelohde (200 μm) viscometer at a concentration of 0.2 g/dL in sulfuric acid (H_2SO_4) at 30.0 °C. Aliquots of polymer solution were precipitated in water and neutralized with 0.1 N ammonium hydroxide. After thoroughly washing with water, the samples were dried under vacuum overnight at 120 °C and then dissolved in H_2SO_4 using a mechanical shaker. Reported IV values are an average of three separate measurements and were calculated as previously reported.[38]

The PA contents in the membranes were obtained via titration using a Metrohm 716 DMS Titrino automated titrater and a standardized 0.1 N sodium hydroxide solution following procedures reported previously.[39] PA concentrations were expressed as moles of PA per mole benzimidazole.

Ionic conductivities were measured using a quadra-probe alternating current impedance method which utilized a Zahner IM6e spectrometer operating in the frequency range of 1 Hz to 100 kHz. A rectangular section of the polymer membrane was cut with the dimensions of 3.5 × 7.0 cm^2 and was placed into a polysulfone cell connected to four platinum wire current collectors. Current was supplied to the cell through two outer electrodes which were set 6.0 cm apart, while the potential drop was measured by two inner electrodes which were set 2.0 cm apart. The inner and outer electrodes of the cell were positioned on alternating sides of the polymer membrane to obtain through-plane bulk measurements of ionic conductivity. A programmable oven was used to house the cell so that a measure of the temperature dependence of the proton conductivity for the membrane could be obtained. Two series of measurements of the conductivity were conducted subsequently. The first series of measurements were conducted from ambient temperature to 180 °C, at intervals of 20 °C, with a 15 min pause at each temperature interval for thermal equilibrium prior to measurement. The second series of measurements were subsequently conducted in the same manner to obtain the ionic conductivity of the membranes under anhydrous conditions. A Nyquist plot was constructed to fit the experimental curve of the resistance across the frequency range. The conductivities were calculated at different temperatures from the membrane resistance obtained using the following equation:

$$\sigma = \frac{D}{(W \times T \times R)} \quad (1)$$

where σ is the ionic conductivity, R is the resistance measured, W and T are the width and thickness of the membrane, respectively, and D is the distance between the two inner electrodes.

Glass transition (T_g) analysis was conducted using a DMA (TA Instruments, model ARES-RSA3). Polymer films cast from PPA solution were heated (~60 °C) and stirred in deionized water for several days to remove the internal PA of the film. The pH of the water was monitored and water exchange was conducted over the duration of preparation until a neutral pH was observed. Polymer films of 35 × 6 × 1.5 mm^3 ($L \times W \times T$), were cut and hot pressed at 140 °C for approximately 1.5 h. Samples were then clamped on the film tension clamp of the precalibrated instrument. Scans were conducted from 300 to 550 °C at a heating rate of 5 °C/min. The storage modulus (E'), loss modulus (E'') and tan δ values were measured at a constant frequency of 1 Hz, using autotension with an initial strain of 0.08% and initial static force of 20 g.

MEA Fabrication and Fuel Cell Testing

MEAs were fabricated by hot pressing a membrane (~20% compression) sample between two platinum-doped carbon electrodes, and were 50 cm^2 in area (45.15 cm^2 active area). Gas diffusion electrodes, with a platinum loading of 1.0 mg/cm^2 on each electrode, were obtained from BASF Fuel Cell. A Kapton framework was also incorporated to add stability to the MEA, and to allow handling without damaging the MEA. The MEA was placed into a single-cell fuel cell apparatus for testing. The gas flow plates used were graphite with dual gas channels on the anode and triple gas channels on the cathode. Steel endplates were used to clamp the gas flow plates together. Heating pads were attached to the steel plates to regulate and monitor temperature. A commercially available fuel cell testing station (Fuel Cell Technologies, Inc.) equipped with mass flow regulators was used to conduct and record measurements. Stoichiometric gases were supplied to the anode and cathode at a stoichiometric ratio (hydrogen and air) of 1.2 and 2.0, respectively, without applied backpressure. Fuel/oxidant studies were performed without humidification.

RESULTS AND DISCUSSION

The random copolymers of AB-PBI and *i*-AB-PBI are unique in that there is no variation in chemical composition or functionality of the polymer repeat unit across the compositional spectrum. All polymers in this study are structurally comprised of repeating 2,5-benzimidazole units. The differences lie in the orientation of the benzimidazole units. Previous work has shown that sequence isomerism of the polymer main chain significantly affected properties of the resulting

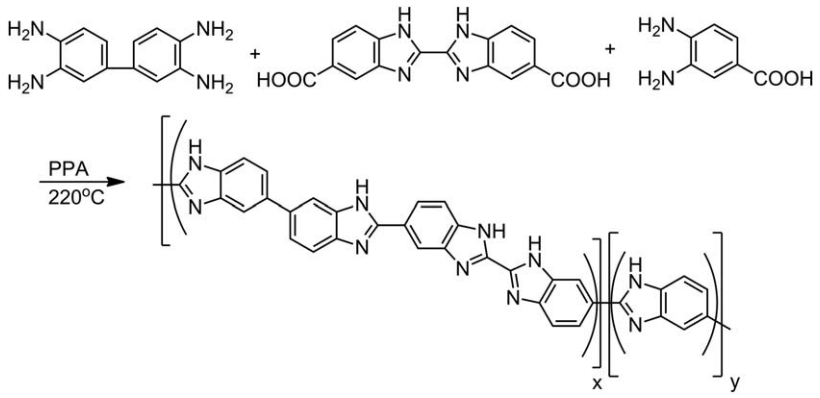

SCHEME 1 Synthesis of random AB-PBI polymers.

polymer.[34] Moreover, the r-AB-PBI system introduces disorder through the random orientation of the benzimidazole unit in the polymer sequence when compared to the ordered structures of both AB-PBI and *i*-AB-PBI.

Polymerization of Random AB-PBI Copolymers (r-AB-PBI)

Using the previously reported novel bisbenzimidazole monomer,[34] 2,2′-bisbenzimidazole-5,5′-dicarboxylic acid, along with recrystallized 3,4-diaminobenzoic acid and 3,3′,4,4′-tetraaminobiphenyl, in PPA solution, random copolymers of AB-PBI and *i*-AB-PBI were prepared, as shown in Scheme 1. Assuming the principal of equal reactivity,[40] copolymerization of the above-mentioned monomers results in a randomized benzimidazole sequence, that is, a polymer chain composed of repeating 2,5-benzimidazole units with a random sequence of 2,5 2,2, and 5,5 linkages. Polymerization of these monomers is an AA-BB-AB type polycondensation polymerization, and as defined by the Carother's equation[41] an exact stoichiometric ratio is needed between AA and BB monomers to achieve high-molecular weight polymer. By variation of AB monomer ratio, random copolymer compositions between 0 and 100 mol % of AB-PBI and *i*-AB-PBI were synthesized. Polymerization conditions were adjusted from the previously reported synthetic conditions[34] of the corresponding homo-polymers as composition was varied. Random copolymers of AB-PBI and *i*-AB-PBI obtained had inherent viscosities ranging between 2.13 and 3.48 dL/g indicating that high-molecular weight polymers were obtained. Resulting gel films from the PPA process were fabricated and evaluated for high-temperature PEM fuel cell use.

Membrane Formation and Properties

Polymer solutions were directly cast at 220 °C on to heated glass plates (120 °C oven temperature) using a 20 mil (508 μm) casting blade. The solutions then underwent a sol-to-gel transition as the PPA of the membrane hydrolyzed into PA and the system temperature decreased to ambient conditions. The membrane composition data obtained from titration shows that the typical compositions of r-AB-PBI membranes (as cast) prepared using the PPA process are greater than 50 wt % PA and have a polymer content ranging from 6.22 to 11.61 wt %. Mechanical property evaluations of the r-AB-PBI doped membranes typically yielded Young's moduli ranging from 0.3 to 1.6 MPa and tensile strengths between 0.3 and 1.0 MPa. Membrane composition data along with other significant properties for r-AB-PBI films are shown in Table 1.

Thermal Analysis

PBI type polymers are well-known for their high thermal stabilities resulting from their fully aromatic structure and polymer chain rigidity.[19,42–44] Thermal evaluations of r-AB-PBI copolymers were conducted via TGA from ambient temperature to 750 °C with a heating rate of 5 °C/min in nitrogen. TGA curves and thermal data for several samples of the r-AB-PBI copolymers, along with AB-PBI and *i*-AB-PBI are shown in Figure 2 and Table 2, respectively. Two weight loss regions were observed in the analysis: an initial weight loss region between 100–200 °C, and a decomposition region above 600 °C. The initial weight loss region between 100 and 200 °C results from loss of bound water, despite thorough drying under vacuum at 120 °C. PBI polymers are very hygroscopic and have been shown to absorb approximately 10–15% (by weight) of water, even in short sample handling times.[45] Thermal degradation of the polymer backbone is observed between 580 and 600 °C. Above 600 °C, rapid weight loss is observed. Figure 2 and Table 2 show that $<$10% weight loss is observed at 570 and 600 °C for AB-PBI and *i*-AB-PBI, respectively, indicating the high thermal stabilities of ordered PBIs. Randomized PBIs samples showed slightly lower thermal stability and a higher degradation rate, as would be expected from disrupted chain packing. The randomized PBIs also showed an unusual drop between 200 and 300 °C that was not observed in the corresponding homopolymers. All samples were then investigated using TGA-MS to analyze the off-gas in that temperature range. The TGA-MS analysis showed loss of water and trace amounts of residual DMSO solvent used in monomer purification. TGA curves of AB-PBI, *i*-AB-PBI, and r-AB-PBI suggest

TABLE 1 Characterization Results for Random AB-PBI

	Composition *i*-AB:AB		Monomer charge (wt %)	I.V.	Membrane composition (wt %)			Mol PA/Mol BI	Anhydrous conductivity 180 °C (S/cm)
	i-AB	AB			PA	H_2O	Polymer		
1	100	0	6.21	3.05	54.98	37.76	7.26	9.09	0.202
2	90	10	5.96	2.27	52.98	38.8	8.23	7.63	0.133
3*	90	10	5.50	2.13	58.12	33.69	8.19	11.05	NA
4	80	20	6.01	2.26	58.13	35.66	6.22	9.64	0.059
5	70	30	4.50	3.38	54.81	38.03	7.16	11.09	0.2
6*	70	30	5.84	2.67	54.49	39.94	9.57	7.19	NA
7	60	40	4.97	3.48	59.17	34.48	6.35	5.11	0.18
8	50	50	5.48	2.59	64.99	24.29	10.72	7.51	0.217
9	40	60	4.96	3.11	49.38	39.01	11.61	6.5	0.112
10	30	70	5.45	3.37	55.09	36.21	8.7	7.7	0.146
11	20	80	3.61	2.30	56.17	33.58	10.25	8.65	0.0878
12	10	90	3.05	3.23	58.3	32.73	8.97	9.09	0.219
13*	0	100	2.76	4.63	62.17	34.36	3.47	7.63	NA

*Samples obtained were not suitable for high temperature proton conductivity measurements; I.V., inherent viscosity, BI, benzimidazole.

that thermal stability is inversely proportional to the randomization of benzimidazole sequence.

Glass Transition Temperature (T_g) Effects of r-AB-PBI Copolymers

DSC measurements were conducted over the compositional range of the copolymers as an initial method of observing T_g. The DSC thermograms revealed information about the glass transitions, but were not prominent enough for accurate interpretation. Therefore, DMA measurements were conducted to precisely determine the glass transition temperatures of the copolymers. Glass transition events were clearly observed as shown in Figure 3 which shows a representative DMA tan δ plot of a 30:70 (*i*-AB:AB) r-AB-PBI. As the compositional spectrum of the copolymers was evaluated, an anomalous T_g effect was observed. The T_g values for r-AB-PBI compositions are shown in Figure 4. The theoretical T_g values for the r-AB-PBI were calculated by the Fox equation,[46] eq 2.

$$\frac{1}{T_g} = \frac{W_1}{T_{g1}} + \frac{W_2}{T_{g2}} \quad (2)$$

where W_1 and W_2 are the weight fractions and T_{g1} and T_{g2} are the glass transition temperatures of the corresponding homopolymers. The experimental values obtained as compared to theoretical T_g values, show a sharp deviation from the predicted values corresponding with the region of highest randomization. The DMA results were confirmed when new polymer batches were evaluated and the measurements were reproduced. The deviation of the experimentally

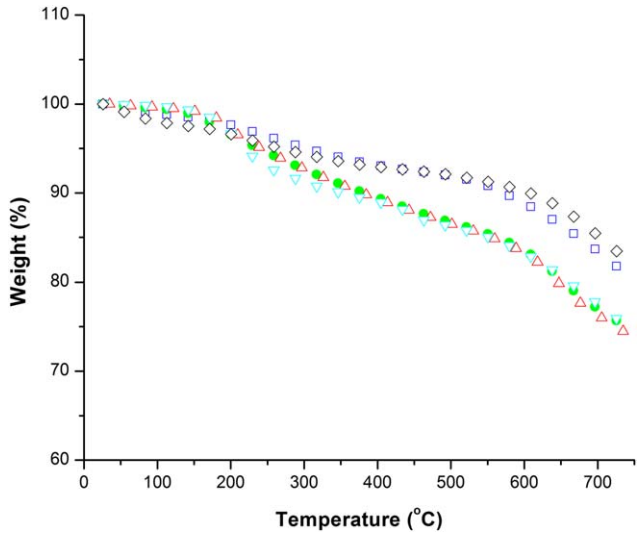

FIGURE 2 Thermal gravimetric analysis. Squares: i-AB-PBI, dot: 70:30 i-AB:AB, upward triangle: 50:50 i-AB:AB, downward triangle: 30:70 i-AB:AB, diamond: AB-PBI. [Color figure can be viewed in the online issue, which is available at wileyonline library.com.]

TABLE 2 Thermal Properties for AB-PBI Polymers Under Nitrogen

Sample	T_g (°C)	T_{d5} (°C)	T_{d10} (°C)
i-AB-PBI	500	304	572
70:30 r-AB	512	238	381
50:50 r-AB	515	242	378
30:70 r-AB	379	220	351
AB-PBI	520	268	606

Td5, temperature at 5% weight loss; Td10, temperature at 10% weight loss.

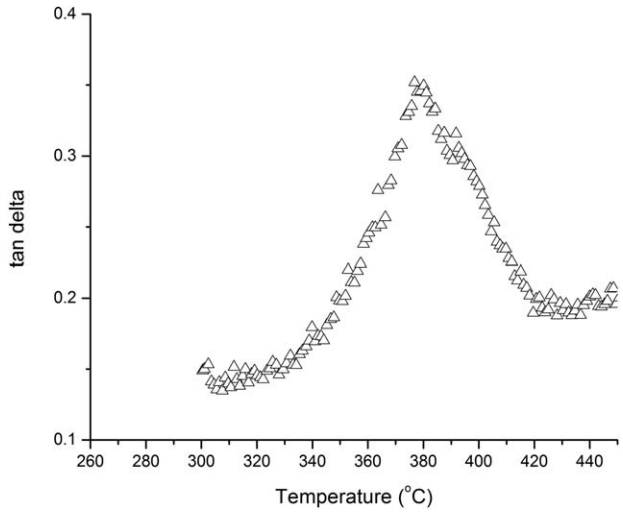

FIGURE 3 DMA tan δ plot of r-AB-PBI (30:70 i-AB:AB).

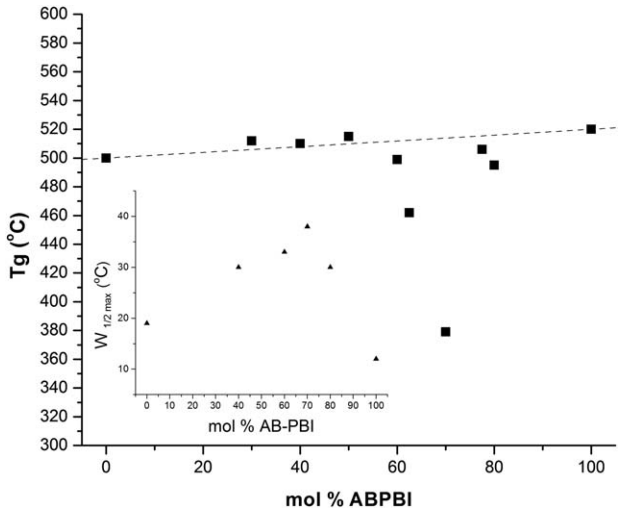

FIGURE 4 Effect of copolymer composition on glass transition temperature, T_g. Repeat measurements were conducted and error of ± 1 °C was determined. Dashed line is a calculated plot of the Fox equation. Inset: plot of tan δ peak width at half max with respect to composition.

determined T_g values from those predicted by the Fox equation are unusual, but are not unprecedented in literature.[47–49] Johnston has reviewed sequence distribution glass transition effects in copolymer systems and gave numerous examples of copolymer systems in which a deviation from predicted T_g values using the Fox equation were observed.[50] It was observed that as randomization of the benzimidazole sequence approached a maximum, the T_g of the material was lowered. The lowest T_g value of 379 °C was observed in the compositional region where randomization is maximized, near 20:80 *i*-AB:AB due to weight contribution. This measurement was confirmed using a second sample from a subsequent polymerization. It is surmised that the disrupted regularity of the benzimidazole sequence impacts inter-chain associations and chain packing, resulting in lowered glass transition temperatures. Figure 4 (insert) shows the width of the tan δ peak at half-max, which also supports our conclusion that the randomization lowers the inter-chain association. To further evaluate this effect, other fundamental properties such as solubility were evaluated.

Solubility

PBIs are known for their low solubility and are generally only soluble in aprotic or strong acid solvents.[51] Several attempts to increase the solubility of PBI-type polymers have been made by incorporation of soluble linkages, functionalities, and copolymerizations.[52–56] In this work, the effects of randomization of the benzimidazole sequence on solubility were examined.

Based on the earlier work of Vogel and Marvel[57,58] concerning solubility of PBIs, the solubility of AB-PBI, *i*-AB-PBI, and r-AB-PBI copolymers were evaluated in several common organic solvents. It was found that all of the AB type PBIs have very low solubility in the organic solvents evaluated, however, a change in solubility was observed across the compositional spectrum of r-AB-PBI samples. This change in solubility results from the randomization of benzimidazole sequence as the chemical composition and functionality are not changed in the r-AB-PBI copolymers. The results of the evaluation, illustrating the sequence dependence on solubility, are shown in Table 3. Although the change in solubility is not dramatic, it does show that the orientation of the benzimidazole nitrogen atoms in the polymer main chain effects polymer–solvent interactions. These effects were also noted in the previously reported evaluation of the isomeric AB-PBI.[34] To further evaluate these effects, studies of the proton conductivity of PA doped membranes were conducted.

Conductivity

As previously mentioned, PBI has both proton acceptor and donor sites that contribute to polymer–solvent interactions. These interactions greatly affect the retention of PA in PBI membranes. Since proton conduction is proposed to occur by means of the Grotthuss-type (hopping) mechanism,[59] orientation of benzimidazole motifs along the polymer chain may affect the proton conduction of the material when doped with PA. In the previous work, we have shown that changes in the benzimidazole sequence within the polymer main chain affect the acid retention in the membrane, which in turn affects proton conductivity.[34] In this article, the proton conductivity of several samples across the compositional spectrum of r-AB-PBI were evaluated. AB-PBI homopolymer samples are not shown in the conductivity evaluations because the membranes with high acid content formed from AB-PBI using the PPA process were found to be unstable at temperatures greater than 100 °C, reverting back to the solution state. A trend was observed in the r-AB-PBI samples, indicating that as randomization of the benzimidazole sequence increased, the conductivity of the material was lowered. Figure 5 shows the temperature dependence of the conductivities measured for *i*-AB-PBI and r-AB-PBI samples. Repeat measurements were conducted to determine the error of the measurement and to also confirm the observed

TABLE 3 Solubility Evaluation Results for AB-PBI Polymers

		Qualitative solubility				
Polymer	Polymer IV	DMAc (158 °C)	Formic acid (98 °C)	NMP (195 °C)	DMAc/LiCl (158 °C)	Formic acid/*m*-cresol (98 °C)
i-AB-PBI	3.05	+	++	+	+	++
70:30 r-AB-PBI	2.67	++	+	++	+	+
50:50 r-AB-PBI	2.59	+	++	+	++	+
30:70 r-AB-PBI	3.37	+	++	++	+++	+++
AB-PBI	4.63	+	+++	+	++	++

Solutions were made at 1 wt % and held at temperature for 6 days with constant stirring. DMAc/LiCl (4%) and formic acid/m-cresol (80:20 v/v) were used.

Observations made on hot solutions.
+++, soluble; ++, mostly soluble; +, very little solubility with polymer swelling, –, no solubility.

trend. Moderate to high conductivities were observed for the r-AB-PBI copolymers as compared to previous literature results for AB-PBI with lower amounts of PA dopant.[60] The conductivities of the membranes generally scaled with the PA/BI in the membrane. Several of the compositions were found to have very high proton conductivity (~0.2 S/cm) and indicated these membranes were suitable candidates for high temperature fuel cell applications.

Since conductivity is very closely associated with the electrolyte doping level in PEMs, the relationship between PA retention and r-AB-PBI composition was investigated. Figure 6 shows that compositions above 50 mol % *i*-AB-PBI in AB-PBI copolymers generally retained more PA than compositions below that percentage. Previous work showed that the *i*-AB-PBI membranes were more stable with respect to PA loading than AB-PBI membranes and had a higher acid retention.[34] This correlates with the trend discussed in Figure 5. When conductivity was examined with respect to PA retention, a very clear relationship was observed and is shown in Figure 7. A critical doping level was observed between 7 and 8 mol of PA per moles of benzimidazole. Above this critical level, conductivities of 0.2 S/cm were consistently observed, whereas below this level, the maximum conductivity achieved was 0.1 S/cm. We believe this trend in acid loading, gel stability and proton conductivity correlates with the T_g trend discussed earlier, and is indicative of the difference in chain packing associated with the sequence randomization.

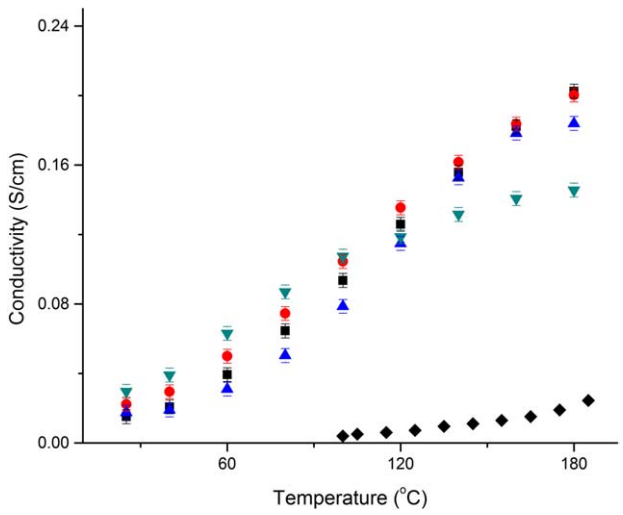

FIGURE 5 Anhydrous conductivity evaluation for r-AB-PBI at 180 °C [squares: *i*-AB-PBI, circles: 70:30 i-AB:AB, triangles: 50:50 *i*-AB:AB, inverted triangle: 30:70 *i*-AB:AB, diamonds: reported literature values for poly(2,5-benzimidazole)(AB-PBI)[60]]. [Color figure can be viewed in the online issue, which is available at wileyonlinelibrary.com.]

Fuel Cell Performance

Fuel cell performance evaluations were conducted on the r-AB-PBI membranes which included polarization curves using a hydrogen/air fuel/oxidant combination over a range of temperatures (120–180 °C). Representative polarization curves are shown for the 60:40 (*i*-AB:AB) r-AB-PBI along with *i*-AB-PBI in Figures 8 and 9, respectively. These two samples were selected since they have similar PA loadings

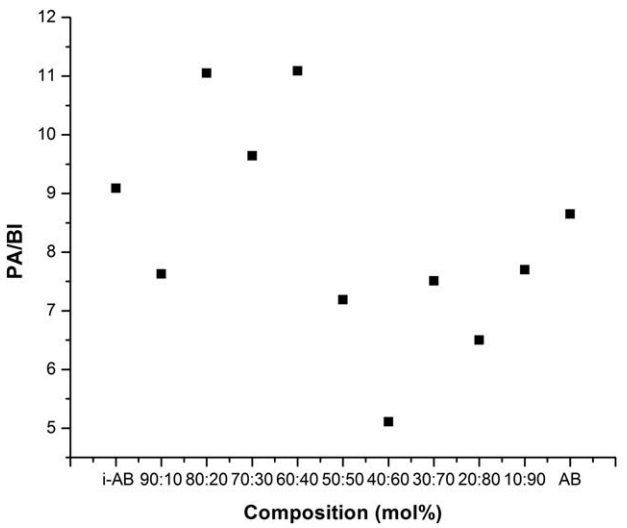

FIGURE 6 Variation of acid loading with copolymer composition for r-AB-PBI copolymers. PA/BI: moles PA per mole of benzimidazole.

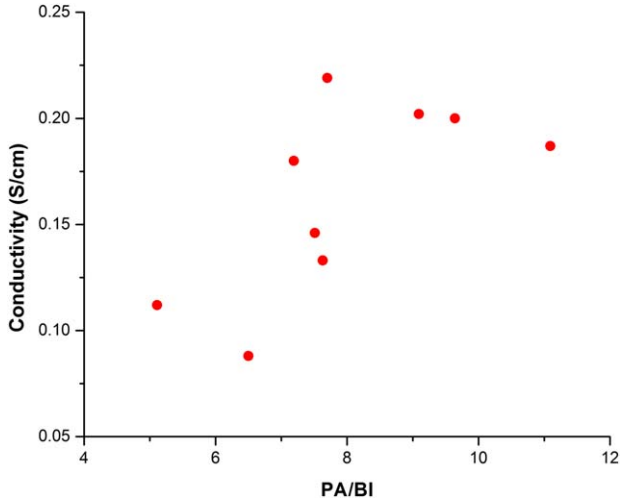

FIGURE 7 Effect of phosphoric acid loading on ionic conductivity at 180 °C for r-AB-PBI copolymers. PA/BI: moles PA per mole of benzimidazole. [Color figure can be viewed in the online issue, which is available at wileyonlinelibrary.com.]

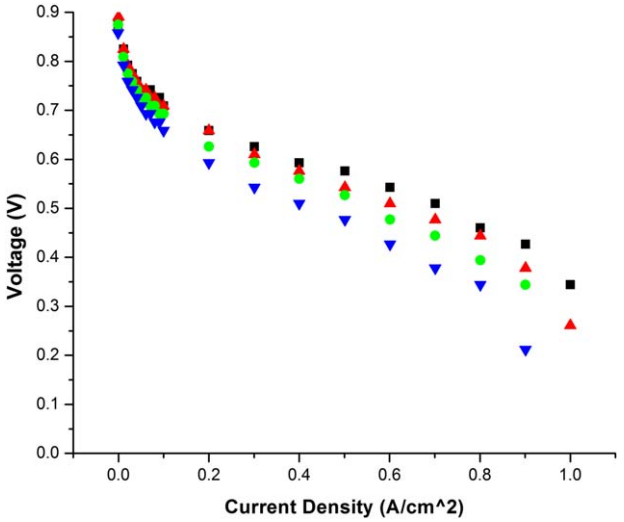

FIGURE 9 Polarization curves for *i*-AB-PBI using H2:Air 1.2:2.0 stoichiometric flows, respectively [squares: 180 °C, triangles: 160 °C, circles: 140 °C, inverted triangles: 120 °C]. [Color figure can be viewed in the online issue, which is available at wileyonlinelibrary.com.]

and similar high temperature anhydrous ionic conductivities. A decrease in performance over the range of temperatures evaluated was observed for the randomized AB-PBI when compared with *i*-AB-PBI and might indicate a change in polymer–PA interactions or an effect of polymer order on the conduction pathways. Lifetime performance studies were conducted on the r-AB-PBI membranes and an average output voltage ranging from 0.5 to 0.6 V at a current density of 0.2 A/cm^2 was observed which appear to be stable over several hundred hours, as shown in Figure 10. A trend in fuel cell performance was observed as the compositional spectrum was shifted towards that of AB-PBI and is shown as the inset of Figure 10. The trend observed for the fuel cell performance in r-AB-PBI compositions correlates directly with the results observed for conductivity.

CONCLUSIONS

A combination of monomer design and copolymerization techniques were used to prepare high molecular weight AB type PBIs comprised of a randomized benzimidazole

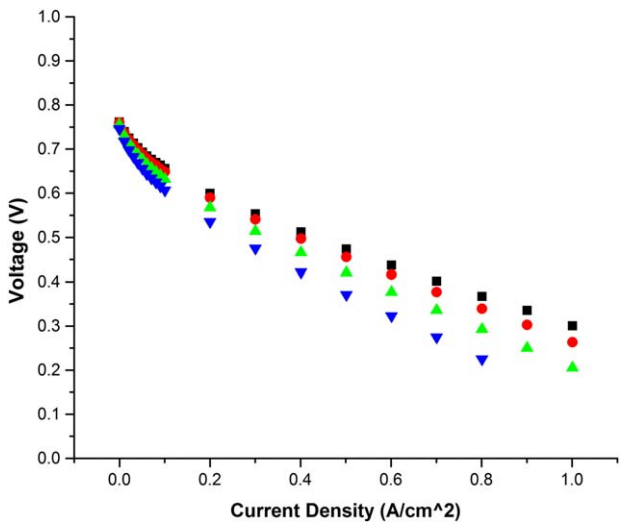

FIGURE 8 Polarization curves for 60:40 *i*-AB-PBI:AB-PBI using H2:Air 1.2:2.0 stoichiometric flows, respectively [squares: 180 °C, circles: 160 °C, triangles: 140 °C, inverted triangles: 120 °C]. [Color figure can be viewed in the online issue, which is available at wileyonlinelibrary.com.]

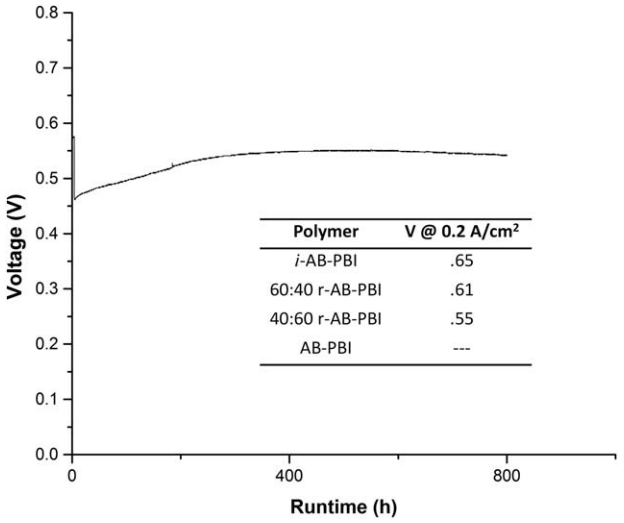

FIGURE 10 Lifetime fuel cell performance of 40:60 (*i*-AB:AB) r-AB-PBI membrane. Inset: fuel cell performance observed over compositional range for the r-AB-PBI copolymer system. Data collected from fuel cells operated at 180 °C supplied with hydrogen/air at 1.2:2.0 stoichiometric flows, respectively, under 1 atm without applied backpressure or humidification.

sequence. Disrupted regularity of sequence in the polymer main chain was found to affect fundamental polymer properties, such as chain packing, solubility, glass transition (T_g) temperatures, as well as membrane properties for high-temperature fuel cell application.

PA doped random co-polymer membranes of AB-PBI and *i*-AB-PBI were developed using the PPA process. Random AB-PBI polymers obtained had inherent viscosities >2.0 dL/g, and formed mechanically robust films. Thermal evaluations of the randomized AB-PBI copolymers showed a slight decrease in thermal stability when compared with the ordered structures of AB-PBI and *i*-AB-PBI. Glass transition (T_g) values measured for the r-AB-PBI showed an unexpected depression when compared with theoretical values, and a maximum T_g depression of 140 °C was observed.

Randomized AB-PBI copolymers showed several differences across the compositional spectrum when compared with the AB-PBI and *i*-AB-PBI homopolymers, indicating primary chemistry and sequence affect properties of both the polymer and membranes derived thereof. A sequence dependence of solubility was observed as well as trends regarding conductivity, PA retention, and fuel cell performance. Random AB-PBI copolymer membranes were evaluated for mechanical integrity, ionic conductivity and fuel cell performance. An output voltage ranging between 0.5 and 0.6 V at 0.2 A/cm^2 for hydrogen/air at an operational temperature of 180 °C was observed for several r-AB-PBI compositions, indicating these materials would be suitable candidates for high temperature fuel cell applications. When comparing films with similar PA doping and conductivity, an effect on fuel cell performance from sequence isomerism was observed. Thus it appears that both high PA loadings and a more ordered polymer structure contribute to high conductivities and membrane properties.

Overall, this unique copolymer series provided an opportunity to evaluate fundamental properties of PBI that would not be achievable in other copolymer systems. Because the copolymers evaluated consist of only repeating 2,5 benzimidazole units, without extraneous functionality or spacers, the fundamental properties of PBI regarding sequence, orientation, and regularity are reported.

ACKNOWLEDGMENTS

BASF Fuel Cell Inc. is especially recognized for financial and technical support of this research. The authors would also like to acknowledge the help of Ben Batchleor and Dr. Dennis Smith at the University of Texas at Dallas for conducting TGA-MS analysis.

REFERENCES AND NOTES

1 B. C. H. Steele, A. Heinzel, *Nature* **2001**, *414*, 345–352.

2 B. C. H. Steele, *J. Mater. Sci.* **2001**, *36*, 1053–1068.

3 H. Ekstrom, B. Lafitte, J. Ihonen, H. Markusson, P. Jacobsson, A. Lundblad, P. Jannasch, G. Lindbergh, *Solid State Ionics* **2007**, *178*, 959–966.

4 G. Qian, B. C. Benicewicz, *ECS Trans.* **2011**, *41*, 1441–1448.

5 P. Jannasch, *Curr. Opin. Colloid Interface Sci.* **2003**, *8*, 96–102.

6 J. Mader, L. Xiao, T. J. Schmidt, B. C. Benicewicz, *Adv. Polym. Sci.* **2008**, *216*, 63–124.

7 S. Yu, L. Xiao, B. C. Benicewicz, *Fuel Cells* **2008**, 3–4, 165–174.

8 C. Shogbon, J. Brousseau, H. Zhang, B. C. Benicewicz, Y. Akpalu, *Macromolecules* **2006**, *39*, 9409–9418.

9 A. Sannigrahi, S. Ghosh, S. Maity, T. Jana, *Polymer* **2010**, *51*, 5929–5941.

10 T. Kojima, *J. Polym. Sci. Polym. Phys. Ed.* **1980**, *18*, 1685–1695.

11 C. B. Shogbon, J. L. Brousseau, H. Zhang, B. C. Benicewicz, Y. Akpalu, *Macromolecules* **2006**, *39*, 9409–9418.

12 A. Sannigrahi, D. Arunbabu, R. M. Sankar, T. Jana, *Macromolecules* **2007**, *40*, 2844–2851.

13 V. Deimede, G. A. Voyiatzis, J. K. Kallitsis, Q. Li, N. Bjerrum, *Macromolecules* **2000**, *33*, 7609–7617.

14 D. Arunbabu, A. Sannigrahi, T. Jana, *J. Phys. Chem. B* **2008**, *112*, 5305–5310.

15 M. Hazarika, T. Jana, *ACS Appl. Mater. Interfaces* **2012**, *4*, 5256–5265.

16 M. Hazarika, *Eur. Polym. J.* **2013**, *49*, 1564–1576.

17 R. Savinell, E. Yeager, D. Tryk, U. Landau, J. Wainright, D. Weng, K. Lux, M. Litt, C. Rogers, *J. Electrochem. Soc.* **1994**, *141*, L46–L48.

18 J. R. P. Jayakody, S. H. Chung, L. Durantino, H. Zhang, L. Xiao, B. C. Benicewicz, S. G. Greenbaum, *J. Electrochem. Soc.* **2007**, *154*, B242–B246.

19 E. W. Choe, D. D. Choe, In Polymeric Materials Encyclopedia; J. C. Salamone, Ed.; CRC Press: New York, **1996**, *17*, 5619–5638.

20 S. R. Samms, S. Wasmus, R. F. Savinell, *J. Electrochem. Soc.* **1996**, *143*, 1225–1232.

21 Q. Li, J. O. Jensen, R. F. Savinell, N. J. Bjerrum, *Prog. Polym. Sci.* **2009**, *34*, 449–477.

22 D. C. Seel, B. C. Benicewicz, L. Xiao, T. J. Schmidt, *Handbook of Fuel Cells* **2009**, *5*, 300–312.

23 A. Sannigrahi, D. Arunbabu, R. M. Sankar, T. Jana, *J. Phys. Chem. B* **2007**, *111*, 12124–12132.

24 M. P. Kulkarni, O. D. Thomas, T. J. Peckhm, S. Holdcroft, *Macromolecules* **2007**, *40*, 983–990.

25 S. Maity; T. Jana, *Macromolecules* **2013**, *46*, 6814–6823.

26 L. Xiao, H. Zhang, T. Jana, E. Scanlon, R. Chen, E. W. Choe, L. S. Ramanathan, S. Yu, B. C. Benicewicz, *Fuel Cells* **2005**, *2*, 287–295.

27 S. Yu, B. C. Benicewicz, *Macromolecules* **2009**, *42*, 8640–8648.

28 S. Kang, C. Zhang, G. Xiao, D. Yan, G. Sun, *J. Membr. Sci.* **2009**, *334*, 91–100.

29 G. Qian, B. C. Benicewicz, *J. Polym. Sci. A* **2009**, *47*, 4064–4073.

30 S. Arindam, G. Sandip, M. Sudhangshu, T. Jana, *Polymer* **2010**, *51*, 5929–5941.

31 F. Ng, B. Bae, K. Miyatake, M. Watanabe, *Chem. Commun.* **2011**, *47*, 8895–8897.

32 J. Mader, B. Benicewicz, *Fuel Cells* **2011**, *2*, 222–237.

33 D. Seel, B. C. Benicewicz, *J. Membr. Sci.* **2012**, 405–406, 57–67.

34 A. Gulledge, B. Gu, B. Benicewicz, *J. Polym. Sci. A* **2012**, *50*, 306–313.

35 L. Xiao, H. Zhang, E. Scanlon, S. L. Ramanathan, E. W. Choe, D. Rogers, T. Apple, B. C. Benicewicz, *Chem. Mater.* **2005**, *17*, 5328–5333.

36 Dictionary of Organic Compounds, 4th ed.; G. Harris, J. R. A. Pollock; R. Stevens, Eds.; Oxford University Press: Oxford, **1965**; Vol. 2, 854.

37 P. J. Flory, *Farad. Discuss. Chem. Soc.* **1974**, *57*, 7–18.

38 J. A. Mader, B. C. Benicewicz, *Macromolecules* **2010**, *43*, 6706–6715.

39 J. A. Mader, B. C. Benicewicz, *Fuel Cells* **2011**, *2*, 212–221.

40 P. Flory, Principles of Polymer Chemistry; Cornell University Press: Ithaca, **1953**, pp 321–322.

41 W. J. Carothers, *J. Am. Chem. Soc.* **1929**, *51*, 2548–2559.

42 E. W. Neuse, *Adv. Polym. Sci.* **1982**, *47*, 1–42.

43 A. Buckley, D. E. Stuetz, G. A. Serad, Encyclopedia of Polymer Science and Technology; Wiley: New York, **1988**; Vol. 11, pp 572–601.

44 T. S. Chung, *Plast. Eng.* **1997**, *41*, 701–731.

45 Q. Li, R. He, R. W. Berg, H. A. Hjuler, N. Bjerrum, *J. Solid State Ionics* **2004**, *168*, 177–185.

46 T. G. Fox, P. J. Flory, *J. Appl. Phys.* **1950**, *21*, 581–591.

47 R. B. Beevers, *Trans. Faraday Soc.* **1962**, *58*, 1465–1472.

48 N. W. Johnston, *J. Macromol. Sci. Chem.* **1973**, *A7*, 531–545.

49 N. W. Johnston, *Polym. Prep. Am. Chem. Soc. Div. Polym. Chem.* **1969**, *10*, 608–614.

50 N. W. Johnston, *J. Macromol. Sci. Rev. Macromol. Chem.* **1976**, *C14*, 215–250.

51 T. Ma, Y. F. Li, S. J. Zhang, F. C. Yang, C. L. Gong, J. J. Zhao, Y. F. Li, *Chin. Chem. Lett.* **2011**, *21*, 976–978.

52 J. R. Klaehn, C. J. Orme, E. S. Peterson, F. F. Stewart, J. M. Urban-Klaehn, *Membr. Sci. Technol. Ser.* **2011**, *14*, 295–307.

53 Z. Liang, X. Jiang, H. Xu, D. Chen, J. Yin, *Macromol. Chem. Phys.* **2009**, *210*, 1632–1639.

54 S. C. Kumbharkar, N. Islam, R. A. Potrekar, U. K. Kharul, *Polymer* **2009**, *50*, 1403–1413.

55 V. V. Korshak, A. A. Izyneev, I. S. Novak, E. M. Etonova, *Doklady Adademii Nauk SSSR* **1975**, *220*, 597–600.

56 S. Maity, A. Sannigrahi, S. Ghosh, T. Jana, *Eur. Polym. J.* **2013**, *49*, 2280–2292.

57 H. Vogel, C. S. Marvel, *J. Polym. Sci.* **1961**, *50*, 511–539.

58 H. Vogel, C. S. Marvel, *J. Polym. Sci. Part A* **1963**, *1*, 1531–1541.

59 N. Agmon, *Chem. Phys. Lett.* **1995**, *244*, 456–462.

60 J. A. Asensio, P. Gomez-Romero, *Fuel Cells* **2005**, *5*, 336–343.